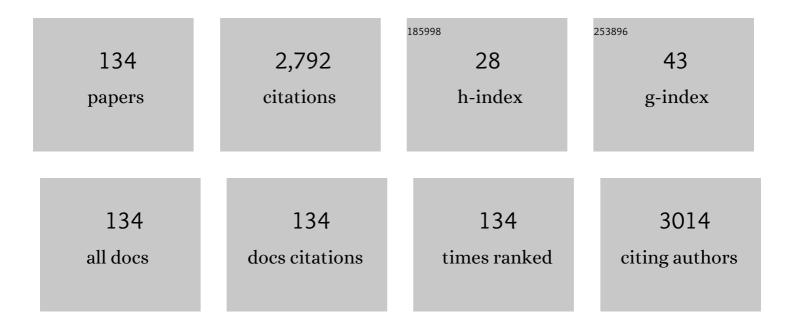
Zhong-Tao Jiang

List of Publications by Year in descending order

Source: https://exaly.com/author-pdf/4417129/publications.pdf Version: 2024-02-01



#	Article	IF	CITATIONS
1	Molybdenum nitrides from structures to industrial applications. Reviews in Chemical Engineering, 2023, 39, 329-361.	2.3	7
2	Structural, surface electronic bonding, optical, and mechanical features of sputtering deposited CrNiN coatings with Si and Al additives. Materials Chemistry and Physics, 2022, 277, 125289.	2.0	5
3	How does biochar aging affect NH3 volatilization and GHGs emissions from agricultural soils?. Environmental Pollution, 2022, 294, 118598.	3.7	36
4	Thermal stability, mechanical properties, and tribological performance of TiAlXN coatings: understanding the effects of alloying additions. Journal of Materials Research and Technology, 2022, 17, 961-1012.	2.6	30
5	Factors Determining the Resistive Switching Behavior of Transparent InGaZnOâ€Based Memristors. Physica Status Solidi - Rapid Research Letters, 2022, 16, .	1.2	10
6	Hydrochar amendments stimulate soil nitrous oxide emission by increasing production of hydroxyl radicals and shifting nitrogen functional genesÂin the short term: A culture experiment. Chemosphere, 2022, 302, 134771.	4.2	7
7	Repurposing N-Doped Grape Marc for the Fabrication of Supercapacitors with Theoretical and Machine Learning Models. Nanomaterials, 2022, 12, 1847.	1.9	20
8	Sliding wear of electro-carburized mild steel with different microstructures. Tribology - Materials, Surfaces and Interfaces, 2021, 15, 213-228.	0.6	3
9	A Short Review on the Phase Structures, Oxidation Kinetics, and Mechanical Properties of Complex Ti-Al Alloys. Materials, 2021, 14, 1677.	1.3	18
10	A kinetic model for halogenation of the zinc content in franklinite. Applied Surface Science, 2021, 562, 150105.	3.1	13
11	A LaFeO 3 supported naturalâ€clayâ€mineral catalyst for efficient pyrolysis of polypropylene plastic material. Asia-Pacific Journal of Chemical Engineering, 2021, 16, e2695.	0.8	4
12	High temperature (up to 1200°C) thermal-mechanical stability of Si and Ni doped CrN framework coatings. Journal of Materials Research and Technology, 2021, 14, 2406-2419.	2.6	5
13	Very-few-layer graphene obtained from facile two-step shear exfoliation in aqueous solution. Chemical Engineering Science, 2021, 245, 116848.	1.9	10
14	An Insight into Geometries and Catalytic Applications of CeO2 from a DFT Outlook. Molecules, 2021, 26, 6485.	1.7	14
15	Formation of phenoxy-type Environmental Persistent Free Radicals (EPFRs) from dissociative adsorption of phenol on Cu/Fe and their partial oxides. Chemosphere, 2020, 240, 124921.	4.2	17
16	Factors controlling conductivity of PEDOT deposited using oxidative chemical vapor deposition. Applied Surface Science, 2020, 501, 144105.	3.1	20
17	Influence of the variation in the Hubbard parameter (<i>U</i>) on activation energies of CeO ₂ -catalysed reactions. Canadian Journal of Physics, 2020, 98, 385-389.	0.4	7
18	Physico-chemical properties of CrMoN coatings - combined experimental and computational studies. Thin Solid Films, 2020, 693, 137671.	0.8	13

#	Article	IF	CITATIONS
19	Theoretical study on the adsorption ability of (ZnO)6 cluster for dimethylmercury removal and the influences of the supports and other ions in the adsorption process. Adsorption, 2020, 26, 1335-1344.	1.4	1
20	Sol-gel derived ITO-based bi-layer and tri-layer thin film coatings for organic solar cells applications. Applied Surface Science, 2020, 530, 147164.	3.1	19
21	Tuning the morphology and redox behaviour by varying the concentration of Fe in a CoNiFe ternary oxide heterostructure for hybrid devices. New Journal of Chemistry, 2020, 44, 9921-9932.	1.4	13
22	Mobility of Air-Stable p-type Polythiophene Field-Effect Transistors Fabricated Using Oxidative Chemical Vapor Deposition. Journal of Electronic Materials, 2020, 49, 3465-3471.	1.0	4
23	Co-pyrolysis of polyethylene with products from thermal decomposition of brominated flame retardants. Chemosphere, 2020, 254, 126766.	4.2	8
24	Role of Additives in Electrochemical Deposition of Ternary Metal Oxide Microspheres for Supercapacitor Applications. ACS Omega, 2020, 5, 3405-3417.	1.6	54
25	Selective and sensitive visible-light-prompt photoelectrochemical sensor of Cu2+ based on CdS nanorods modified with Au and graphene quantum dots. Journal of Hazardous Materials, 2020, 391, 122248.	6.5	29
26	Biocompatibility study of multi-layered hydroxyapatite coatings synthesized on Ti-6Al-4V alloys by RF magnetron sputtering for prosthetic-orthopaedic implant applications. Applied Surface Science, 2019, 463, 292-299.	3.1	42
27	High temperature in-situ phase stability of sputtered TiAlxN coatings. Journal of Alloys and Compounds, 2019, 786, 507-514.	2.8	6
28	A first-principles study of the electronic, structural, and optical properties of CrN and Mo:CrN clusters. Ceramics International, 2019, 45, 17094-17102.	2.3	4
29	Elucidating the surface geometric design of hydrophobic Australian Eucalyptus leaves: experimental and modeling studies. Heliyon, 2019, 5, e01316.	1.4	2
30	Work function investigations of Al-doped ZnO for band-alignment in electronic and optoelectronic applications. Applied Surface Science, 2019, 484, 990-998.	3.1	37
31	Catalytic de-chlorination of products from PVC degradation by magnetite (Fe3O4). Applied Surface Science, 2019, 480, 792-801.	3.1	15
32	Facile synthesis of a nanoporous sea sponge architecture in a binary metal oxide. Nanoscale Advances, 2019, 1, 1880-1892.	2.2	13
33	Surface structural features and optical analysis of nanostructured Cu-oxide thin film coatings coated via the sol-gel dip coating method. Ceramics International, 2019, 45, 12888-12894.	2.3	31
34	Nanorose-like ZnCo2O4 coatings synthesized via sol–gel route: morphology, grain growth and DFT simulations. Journal of Sol-Gel Science and Technology, 2019, 90, 450-464.	1.1	3
35	Studies of annealing impact on the morphological, opto-dielectric and mechanical behaviors of molybdenum-doped CrN coatings. Thin Solid Films, 2019, 677, 119-129.	0.8	5
36	A holistic analysis of surface, chemical bonding states and mechanical properties of sol-gel synthesized CoZn-oxide coatings complemented by finite element modeling. Ceramics International, 2019, 45, 10882-10898.	2.3	5

#	Article	IF	CITATIONS
37	A mechanical and modelling study of magnetron sputtered cerium-titanium oxide film coatings on Si (100). Ceramics International, 2019, 45, 6875-6884.	2.3	5
38	Annealing effects on microstructural, optical, and mechanical properties of sputtered CrN thin film coatings: Experimental studies and finite element modeling. Journal of Alloys and Compounds, 2018, 750, 451-464.	2.8	35
39	Structural, morphological, and optical characterizations of Mo, CrN and Mo:CrN sputtered coatings for potential solar selective applications. Applied Surface Science, 2018, 440, 1001-1010.	3.1	18
40	Solar selective performance of metal nitride/oxynitride based magnetron sputtered thin film coatings: a comprehensive review. Journal of Optics (United Kingdom), 2018, 20, 033001.	1.0	18
41	Novel Approach for Fabricating Transparent and Conducting SWCNTs/ITO Thin Films for Optoelectronic Applications. Journal of Physical Chemistry C, 2018, 122, 3014-3027.	1.5	33
42	Improved mechanical properties of sol-gel derived ITO thin films via Ag doping. Materials Today Communications, 2018, 14, 210-224.	0.9	21
43	Thermo-mechanical properties of cubic lanthanide oxides. Thin Solid Films, 2018, 653, 37-48.	0.8	10
44	Understanding the impacts of Al+3-substitutions on the enhancement of magnetic, dielectric and electrical behaviors of ceramic processed nickel-zinc mixed ferrites: FTIR assisted studies. Materials Research Bulletin, 2018, 97, 444-451.	2.7	22
45	Recycling of zincite (ZnO) <i>via</i> uptake of hydrogen halides. Physical Chemistry Chemical Physics, 2018, 20, 1221-1230.	1.3	26
46	Thermo-mechanical properties of cubic titanium nitride. Molecular Simulation, 2018, 44, 415-423.	0.9	11
47	Catalytic de-halogenation of alkyl halides by copper surfaces. Journal of Environmental Chemical Engineering, 2018, 6, 7214-7224.	3.3	5
48	Development of Organo-Dispersible Graphene Oxide via Pseudo-Surface Modification for Thermally Conductive Green Polymer Composites. ACS Omega, 2018, 3, 18124-18131.	1.6	8
49	Catalytic Hydrogenation of <i>p</i> -Chloronitrobenzene to <i>p</i> -Chloroaniline Mediated by γ-Mo ₂ N. ACS Omega, 2018, 3, 14380-14391.	1.6	15
50	Geometries, electronic properties and stability of molybdenum and tungsten nitrides low-index surfaces. Materials Research Express, 2018, 5, 126402.	0.8	8
51	Hydrodesulfurization of Thiophene over Î ³ -Mo2N catalyst. Molecular Catalysis, 2018, 459, 21-30.	1.0	30
52	Integrated QMMM and Monte Carlo methods for analysis of adsorptive interactions between goethite cluster, carbon nanotubes, and arsenate. International Journal of Quantum Chemistry, 2018, 118, e25653.	1.0	0
53	Surface structural and solar absorptance features of nitrate-based copper-cobalt oxides composite coatings: Experimental studies and molecular dynamic simulation. Ceramics International, 2018, 44, 15274-15280.	2.3	3
54	Influence of DC magnetron sputtering reaction gas on structural and optical characteristics of Ce-oxide thin films. Ceramics International, 2018, 44, 16450-16458.	2.3	17

#	Article	IF	CITATIONS
55	Structural, electronic and thermodynamic properties of bulk and surfaces of terbium dioxide (TbO ₂). Materials Research Express, 2018, 5, 085901.	0.8	9
56	Structural and optical characteristics of pre- and post-annealed sol-gel derived CoCu-oxide coatings. Journal of Alloys and Compounds, 2017, 701, 222-235.	2.8	12
57	Mechanisms governing selective hydrogenation of acetylene over γ-Mo ₂ N surfaces. Catalysis Science and Technology, 2017, 7, 943-960.	2.1	25
58	Reactions of products from thermal degradation of PVC with nanoclusters of $\hat{I}\pm$ -Fe 2 O 3 (hematite). Chemical Engineering Journal, 2017, 323, 396-405.	6.6	24
59	Experimental and predicted mechanical properties of Cr _{1â^'x} Al _x N thin films, at high temperatures, incorporating in situ synchrotron radiation X-ray diffraction and computational modelling. RSC Advances, 2017, 7, 22094-22104.	1.7	16
60	Structure, Stability, and (Non)Reactivity of the Low-Index Surfaces of Crystalline B ₂ O ₃ –l. Journal of Physical Chemistry C, 2017, 121, 11346-11354.	1.5	10
61	Improving the optoelectronic properties of titanium-doped indium tin oxide thin films. Semiconductor Science and Technology, 2017, 32, 065011.	1.0	14
62	Probing the effects of thermal treatment on the electronic structure and mechanical properties of Ti-doped ITO thin films. Journal of Alloys and Compounds, 2017, 721, 333-346.	2.8	16
63	Understanding the adsorptive interactions of arsenate–iron nanoparticles with curved fullerene-like sheets in activated carbon using a quantum mechanics/molecular mechanics computational approach. Physical Chemistry Chemical Physics, 2017, 19, 14262-14268.	1.3	4
64	Study of structural properties and defects of Ni-doped SnO2nanorods as ethanol gas sensors. Nanotechnology, 2017, 28, 265702.	1.3	23
65	Investigation of the post-annealing electromagnetic response of Cu–Co oxide coatings via optical measurement and computational modelling. RSC Advances, 2017, 7, 16826-16835.	1.7	27
66	Electronic properties and stability phase diagrams for cubic BN surfaces. Molecular Simulation, 2017, 43, 267-275.	0.9	4
67	Green synthesis of mesoporous anatase TiO ₂ nanoparticles and their photocatalytic activities. RSC Advances, 2017, 7, 48083-48094.	1.7	118
68	DFTÂ+ U and ab initio atomistic thermodynamics approache for mixed transitional metallic oxides: A case study of CoCu 2 O 3 surface terminations. Materials Chemistry and Physics, 2017, 201, 241-250.	2.0	13
69	Colorimetric and visual dopamine assay based on the use of gold nanorods. Mikrochimica Acta, 2017, 184, 4125-4132.	2.5	17
70	Decomposition of selected chlorinated volatile organic compounds by ceria (CeO ₂). Catalysis Science and Technology, 2017, 7, 3902-3919.	2.1	64
71	Phenol dissociation on pristine and defective graphene. Surface Science, 2017, 657, 10-14.	0.8	4
72	Understanding the shrinkage of optical absorption edges of nanostructured Cd-Zn sulphide films for photothermal applications. Applied Surface Science, 2017, 392, 854-862.	3.1	33

#	Article	IF	CITATIONS
73	Chemical bonding states and solar selective characteristics of unbalanced magnetron sputtered Ti _x M _{1â^'xâ^'y} N _y films. RSC Advances, 2016, 6, 36373-36383.	1.7	34
74	Conversion of NO into N ₂ over γ-Mo ₂ N. Journal of Physical Chemistry C, 2016, 120, 22270-22280.	1.5	17
75	Thermal Recycling of Brominated Flame Retardants with Fe ₂ O ₃ . Journal of Physical Chemistry A, 2016, 120, 6039-6047.	1.1	50
76	Structural, optical, and mechanical properties of cobalt copper oxide coatings synthesized from low concentrations of sol-gel process. Physica Status Solidi (A) Applications and Materials Science, 2016, 213, 3205-3213.	0.8	8
77	Structural Thermal Stability of Graphene Oxide-Doped Copper–Cobalt Oxide Coatings as a Solar Selective Surface. Journal of Materials Science and Technology, 2016, 32, 1179-1191.	5.6	24
78	Thermo-elastic and optical properties of molybdenum nitride. Canadian Journal of Physics, 2016, 94, 902-912.	0.4	11
79	Evaluation of different chemical adjuvants on an avian influenza H6 DNA vaccine in chickens. Avian Pathology, 2016, 45, 649-656.	0.8	5
80	NEXAFS N K -edge study of the bonding structure on Al/Si doped sputtered CrN coatings. Journal of Alloys and Compounds, 2016, 661, 268-273.	2.8	13
81	Effects of annealing temperatures on the morphological, mechanical, surface chemical bonding, and solar selectivity properties of sputtered TiAlSiN thin films. Journal of Alloys and Compounds, 2016, 671, 254-266.	2.8	36
82	Double-sided F and Cl adsorptions on graphene at various atomic ratios: Geometric, orientation and electronic structure aspects. Applied Surface Science, 2016, 373, 65-72.	3.1	13
83	Predicting high temperature mechanical properties of CrN and CrAlN coatings from in-situ synchrotron radiation X-ray diffraction. Thin Solid Films, 2016, 599, 98-103.	0.8	17
84	Interaction of Oxygen with α-Rhombohedral Boron (001) Surface. Journal of Physical Chemistry C, 2016, 120, 5968-5979.	1.5	3
85	Trends of elemental adsorption on graphene. Canadian Journal of Physics, 2016, 94, 437-447.	0.4	10
86	Probing the interactions of phenol with oxygenated functional groups on curved fullerene-like sheets in activated carbon. Physical Chemistry Chemical Physics, 2016, 18, 3700-3705.	1.3	10
87	Geometrical and orientational investigations on the electronic structure of graphene with adsorbed aluminium or silicon. Materials and Design, 2016, 89, 27-35.	3.3	6
88	Towards a better understanding of the geometrical and orientational aspects of the electronic structure of halogens (F–I) adsorption on graphene. Applied Surface Science, 2015, 356, 370-377.	3.1	9
89	Influence of different extrusion processes on mechanical properties of magnesium alloy. Journal of Magnesium and Alloys, 2014, 2, 220-224.	5.5	36
90	Surface and interface analysis of poly-hydroxyethylmethacrylate-coated anodic aluminium oxide membranes. Applied Surface Science, 2014, 289, 560-563.	3.1	14

#	Article	IF	CITATIONS
91	Crystallinity and morphological evolution of hydrothermally synthesized potassium manganese oxide nanowires. Ceramics International, 2014, 40, 1245-1250.	2.3	8
92	Tailoring the physicochemical and mechanical properties of optical copper–cobalt oxide thin films through annealing treatment. Surface and Coatings Technology, 2014, 239, 212-221.	2.2	40
93	The structures and thermodynamic stability of copper(<scp>ii</scp>) chloride surfaces. Physical Chemistry Chemical Physics, 2014, 16, 24209-24215.	1.3	13
94	Understanding Local Bonding Structures of Ni-Doped Chromium Nitride Coatings through Synchrotron Radiation NEXAFS Spectroscopy. Journal of Physical Chemistry C, 2014, 118, 18573-18579.	1.5	13
95	Optical properties and thermal durability of copper cobalt oxide thin film coatings with integrated silica antireflection layer. Ceramics International, 2014, 40, 16569-16575.	2.3	26
96	Enhancing toughness of CrN coatings by Ni addition for safety-critical applications. Materials Science & Engineering A: Structural Materials: Properties, Microstructure and Processing, 2014, 596, 264-274.	2.6	46
97	Review of Sol–Gel Derived Mixed Metal Oxide Thin Film Coatings with the Addition of Carbon Materials for Selective Surface Applications. Journal of Advanced Physics, 2014, 3, 179-193.	0.4	19
98	Surface Electronic Structure and Mechanical Characteristics of Copper–Cobalt Oxide Thin Film Coatings: Soft X-ray Synchrotron Radiation Spectroscopic Analyses and Modeling. Journal of Physical Chemistry C, 2013, 117, 16457-16467.	1.5	35
99	Characterization of silicon nanowires grown on silicon, stainless steel and indium tin oxide substrates. Applied Physics A: Materials Science and Processing, 2013, 113, 723-728.	1.1	6
100	The nature and role of passive films in controlling the corrosion resistance of MoSi2-based nanocomposite coatings. Journal of Materials Chemistry A, 2013, 1, 10281.	5.2	23
101	Near-edge X-ray absorption fine structure studies of Cr1â^'xMxN coatings. Journal of Alloys and Compounds, 2013, 578, 362-368.	2.8	12
102	Solar absorptance of copper–cobalt oxide thin film coatings with nano-size, grain-like morphology: Optimization and synchrotron radiation XPS studies. Applied Surface Science, 2013, 275, 127-135.	3.1	168
103	A critical role for Al in regulating the corrosion resistance of nanocrystalline Mo(Si _{1â^'x} Al _x 2films. Journal of Materials Chemistry, 2012, 22, 2596-2606.	6.7	17
104	Designing superhard, self-toughening CrAlN coatings through grain boundary engineering. Acta Materialia, 2012, 60, 5735-5744.	3.8	108
105	Optical and mechanical characterization of novel cobalt-based metal oxide thin films synthesized using sol–gel dip-coating method. Surface and Coatings Technology, 2012, 207, 367-374.	2.2	58
106	Corrosion―and Damageâ€Resistant Nitride Coatings for Steel. Journal of the American Ceramic Society, 2012, 95, 2997-3004.	1.9	7
107	Corrosion behaviour of nanocomposite TiSiN coatings on steel substrates. Corrosion Science, 2011, 53, 3678-3687.	3.0	46
108	Hydrothermal synthesis of cubic α-Fe2O3 microparticles using glycine: Surface characterization, reaction mechanism and electrochemical activity. Journal of Alloys and Compounds, 2011, 509, 9821-9825.	2.8	46

#	Article	IF	CITATIONS
109	Effect of dilute gelatine on the ultrasonic thermally assisted synthesis of nano hydroxyapatite. Ultrasonics Sonochemistry, 2011, 18, 697-703.	3.8	27
110	Development of a Nano-vaccine against a Wild Bird H6N2 Avian Influenza Virus. Procedia in Vaccinology, 2010, 2, 40-43.	0.4	4
111	Synthesis and characterisation of nanohydroxyapatite using an ultrasound assisted method. Ultrasonics Sonochemistry, 2009, 16, 469-474.	3.8	141
112	An in situ electrochemical impedance spectroscopy/synchrotron radiation grazing incidence X-ray diffraction study of the influence of acetate on the carbon dioxide corrosion of mild steel. Electrochimica Acta, 2007, 52, 3746-3750.	2.6	40
113	An in situ chronoamperometry/synchrotron radiation grazing incidence X-ray diffraction study of the electrochemical oxidation of pyrite in chloride media. Electrochemistry Communications, 2006, 8, 1661-1664.	2.3	13
114	In situ electrochemical impedance spectroscopy/synchrotron radiation grazing incidence X-ray diffraction—A powerful new technique for the characterization of electrochemical surfaces and interfaces. Electrochimica Acta, 2006, 51, 5920-5925.	2.6	18
115	In situ synchrotron radiation grazing incidence X-ray diffraction—A powerful technique for the characterization of solid-state ion-selective electrode surfaces. Electrochimica Acta, 2006, 51, 4886-4891.	2.6	12
116	Response Mechanisms and New Approaches with Solid-State Ion-Selective Electrodes: A Powerful Multitechnique Materials Characterization Approach. Electroanalysis, 2006, 18, 1273-1281.	1.5	3
117	An In Situ Synchrotron Radiation Grazing Incidence X-Ray Diffraction Study of Carbon Dioxide Corrosion. Journal of the Electrochemical Society, 2005, 152, B389.	1.3	45
118	The Ag M5N45N45 Auger photoelectron coincidence spectra of disordered Ag0.5Pd0.5 alloy. Journal of Electron Spectroscopy and Related Phenomena, 2003, 130, 33-41.	0.8	12
119	Line structure in photoelectron and Auger electron spectra of CuOx/Cu and Cu by Auger photoelectron coincidence spectroscopy (APECS). Surface and Interface Analysis, 2001, 31, 287-290.	0.8	20
120	Asymmetric broadening of the Cu 2p3/2 photoelectron line. Surface Science, 2000, 466, L807-L810.	0.8	12
121	Measurement and Calculation of Optical Band Gap of Chromium Aluminum Oxide Films. Japanese Journal of Applied Physics, 2000, 39, 4820-4825.	0.8	70
122	Spectroellipsometric characterization of SIMOX with nanometre-thick top Si layers. Thin Solid Films, 1998, 313-314, 264-269.	0.8	4
123	Spectroellipsometric characterization of thin silicon nitride films. Thin Solid Films, 1998, 313-314, 298-302.	0.8	2
124	A Study of Cr–Al Oxides for Single-Layer Halftone Phase-Shifting Masks for Deep-Ultraviolet Region Photolithography. Japanese Journal of Applied Physics, 1998, 37, 4008-4013.	0.8	13
125	Fluorinated silicon nitride film for the bottom antireflective layer in quarter micron optical lithography. Semiconductor Science and Technology, 1997, 12, 921-926.	1.0	2
126	Mass spectroscopic study for vaporization characteristics of Ba(TMHD)2 and Sr(TMHD)2 in electron cyclotron resonance-plasma enhanced metal organic chemical vapor deposition. Journal of Vacuum Science and Technology A: Vacuum, Surfaces and Films, 1997, 15, 72-76.	0.9	7

#	Article	IF	CITATIONS
127	Titanium oxide film for the bottom antireflective layer in deep ultraviolet lithography. Applied Optics, 1997, 36, 1482.	2.1	13
128	Simulation and fabrication of attenuated phase-shifting masks: CrF_x. Applied Optics, 1997, 36, 7247.	2.1	10
129	Title is missing!. Journal of Materials Science, 1997, 32, 1213-1219.	1.7	32
130	Effects of gas ring position and mesh introduction on film quality and thickness uniformity. Materials Science and Engineering B: Solid-State Materials for Advanced Technology, 1997, 45, 98-101.	1.7	9
131	Single-layer halftone phase-shifting masks for DUV microlithography: optical property simulation and chromium compound film preparation. Applied Surface Science, 1997, 113-114, 680-684.	3.1	5
132	Dependence of the properties of (SrxTi1â^'x)O3 thin films deposited by plasma-enhanced metal–organic chemical vapor deposition on electron cyclotron resonance plasma. Thin Solid Films, 1997, 301, 154-161.	0.8	9
133	Preparation and Characterization of (Sr1â^'xTix)O3 and (Ba1â^'xSrx)TiO3 Thin Films using ECR Plasma Assisted MOCVD. Materials Research Society Symposia Proceedings, 1996, 433, 9.	0.1	8
134	Optical property simulation of single-layer halftone phaseshifting masks for DUV microlithography. Semiconductor Science and Technology, 1996, 11, 1450-1455.	1.0	6